Journal of Applied Polymer Science

Characterization and Mechanical Properties of Exfoliated Graphite Nanoplatelets Reinforced Polyethylene Terephthalate/Polypropylene Composites

I. M. Inuwa,[1] Azman Hassan,[1] S. A. Samsudin,[1] M. K. Mohamad Haafiz,[1,2] M. Jawaid,[3] K. Majeed,[1] N. C. Abdul Razak[1]

[1]Department of Polymer Engineering, Faculty of Chemical Engineering, Universiti Teknologi Malaysia, Skudai Johor Bahru, Malaysia

[2]School of Industrial Technology, Universiti Sains Malaysia, Penang, Malaysia

[3]Department of Biocomposites Technology Institute of Tropical Forestry and Forest Products (INTROP), Universiti Putra Malaysia, Selangor, Malaysia

Correspondence to: A. Hassan (E-mail: azmanh@cheme.utm.my)

ABSTRACT: Recently, graphene and its derivatives have been used to develop polymer composites with improved or multifunctional properties. Exfoliated graphite nanoplatelets (GNP) reinforced composite materials based on blend of polyethylene terephthalate (PET), and polypropylene (PP) compatibilized with styrene–ethylene–butylene–styrene-g-maleic anhydride is prepared by melt extrusion followed by injection molding. Characterization of the composites' microstructure and morphology was conducted using field emission scanning electron microscopy, transmission electron microscopy (TEM), X-ray diffraction analysis (XRD), and Fourier transform infrared spectroscopy (FTIR). Tensile and impact strengths of test specimens were evaluated and the results showed maximum values at 3phr GNP in both the cases. Morphological studies showed that the GNPs were uniformly dispersed within the matrix. Results from XRD analysis showed uniformly dispersed GNPs, which may not have been substantially exfoliated. FTIR spectroscopy did not show any significant change in the peak positions to suggest definitive chemical interaction between GNP and the matrix. © 2014 Wiley Periodicals, Inc. J. Appl. Polym. Sci. **2014**, *131*, 40582.

KEYWORDS: blends; compatibilization; composites; mechanical properties; polyolefins

Received 1 November 2013; accepted 11 February 2014
DOI: 10.1002/app.40582

INTRODUCTION

Following the highly celebrated isolation of graphene in 2004, a plethora of research activities ensued in different aspects of its incredible properties. Presently, research activities into the properties and structure of graphene has moved from curiosity-oriented to application-oriented.[1] Graphene is a monolayer carbon nanoparticle that consists of sp^2 hybridized carbon atoms arranged in hexagonal planar structures. Properties that have endeared this unique material to diverse applications are its exceptional mechanical strength (Young's modulus of 1 TPa, tensile strength of 20 GPa),[2,3] excellent electrical (5,000 S/m)[4] and thermal conductivities (~3,000 W/m.K).[5] Some of the areas in which research activity has blossomed include electrical and electronics devices, fuel, and solar cells and the development of multifunctional nanosized polymer composites (NPC).[6–10]

Among the many types of graphitic nanofiller that have been employed in the development of NPC, exfoliated graphite nanoplatelets (GNP) have become a major focus as new reinforcing filler for the improvement of mechanical,[11–13] thermal and barrier properties of graphene-filled polymeric materials. Low cost of graphite, which is the precursor for GNP, is another factor for its increasing use in the fabrication of NPC.[14] Studies have also shown that GNPs behaved as excellent conductive filler and lowered the percolation threshold of composites. GNP consists of short stacks of graphene sheets, which are characterized by high surface area, high aspect ratio, and platelet geometry. The platelet geometry can provide a tortuous path, which molecules have to follow in order to diffuse through composites. Additional advantages of GNPs over other types of fillers, such as carbon nanotubes, are its moderate cost compared with carbon nanotubes, and ease of processing in composite formulation.[11]

Several methods have been used in the preparation of composites including melt intercalation, *in situ* exfoliation, and solution mixing. Melt intercalation has proven most convenient

Table I. Material Characterization

Material	Trade name	Supplier	Density	Molecular weight	Other properties
PET	EM100	Expet extrusion	–	–	Intrinsic visc = 0.82g/dl
PP	SM240	Titan chemicals	0.9 g/cm^3	25,000 g/mol	MFR= 25 g/10 min
SEBS-g-MAH	Kraton FG1901X	Shell chemical company		Styrene block =7000 g/mol Ethylene/butylene Block = 37,500 g/mol	SEBS grafted with 1.84% MAH

among the three methods from the industrial point of view, as it can be easily adapted to existing general plastic processing equipments such as extruders and injection-molding machines. The high amount of shear and heat required to exfoliate nanofillers in matrix can only be generated by melt blending. On the contrary, *in situ* polymerization method is somehow complex and restricted to some polymer types, whereas solution method requires large amounts of solvent, which is difficult to reclaim and with added cost. Many studies have been reported in which direct melt-blending technique was used to disperse graphene in polymer matrix.[15–17] In a recent study, Fasihi et al.[18] reported that solid-state milling followed by low-temperature melt mixing have resulted in high-degree exfoliation of expanded graphite in polypropylene (PP) composites. Melt mixing and solution methods have been compared with coating technique in the preparation of polyethersulphone/exfoliated GNP composites where it is shown that the coating followed by melt injection method is more effective than polymer solution or melt mixing in preserving the platelets morphology and increase in electrical conductivity of the prepared composites,[19] albeit more expensive and extra procedural step is required.

Engineering thermoplastics possess superior mechanical, thermal, and chemical properties and hence are finding widespread applications in automobile and electronic industries. Due to growing demand, it is expected that the global revenue for engineering thermoplastics will hit 76.8234 billion dollars by 2017.[20] However, due to the increasing cost of engineering thermoplastics, researchers are now focusing attention toward finding alternatives. Commodity thermoplastics are relatively inexpensive but have lower performance mechanical properties compared with engineering thermoplastics.

Polyethylene terephthalate (PET) is a semicrystalline commodity thermoplastic with good mechanical properties, chemical resistance, thermal stability, low melt viscosity, and spinnability. PET has been used in several fields such as food packaging, film technology, automotive, electrical, beverages containers, and textile fibers. Despite its diversity of applications, PET is known to have poor impact properties, slow rate of crystallization, and moisture absorption, which tend to limit its use in engineering applications.[21–23] To overcome these drawbacks, PET was generally blended with other polyesters such as polybutylene terephthalate and oleifinic polymers. PP is a linear oleifinic commodity thermoplastic with good processability, light weight, and low cost. Its principal applications are in fiber and packaging industries. However, PP is characterized by low stiffness and flexural modulus, and poor thermal properties that make it a poor candidate where these properties are required.[24,25] Blending PET and PP is done to combine the excellent properties of the two polymers and to overcome their individual shortcomings.

Several studies have reported the fabrication and characterization of PET/GNP[13,15,26] and PP/GNP[11,12,27] composites with improved properties. A new approach on nanosized composites studies consists of composites based on the blends of two or more polymeric materials.

Consequently, some studies have reported PET/PP composites based on clay[28] and carbon black[29] with improved mechanical, thermal, and electrical properties. In this study, an attempt has been made to develop nanocomposites based on the blends of PET/PP and GNPs with improved mechanical properties suitable for applications in the automobile industries where engineering thermoplastics are currently predominantly used. This study attempted to expand the areas of applications of PET and PP beyond their traditional use in fiber and packaging industries. To the best of our knowledge, the PET/PP blends reinforced with GNPs have not received any attention in the literature. Melt extrusion and injection molding were employed to fabricate test samples and the morphology; structure and mechanical properties of the samples were investigated. The use of compatibilizer is expected to improve compatibility of the PET/PP blends and aid the dispersion of GNP in the matrix. Aspects of compatibilization of the PET/PP blends with styrene–ethylene–butylene–styrene-g-maleic anhydride (SEBS-g-MAH) have been reported elsewhere.[30]

EXPERIMENTAL

Materials

Exfoliated GNP, GNP-M-5 grade (99.5% carbon), of average diameter 5 μm and average thickness of less than 10 nm were purchased as dry powder from XG Sciences (East Lansing, MI, USA). Extrusion grade PET (EM100) was obtained from Espet Extrusion Sdn Bhd with intrinsic viscosity of 0.82 g/dL. PP, a copolymer grade (SM240) with density of 0.9 g/cm^3 and melt flow index of 25 g/10 min was supplied by Titan chemicals. SEBS-g-MAH grafted with 1.84 wt % of maleic anhydride was supplied by Shell Chemical Company under the trade name of Kraton FG 1901X with ratio of styrene to ethylene/butylene in the triblock copolymer of 30/70 wt %. Details of material specifications are summarized in Table I.

Sample Preparation

PET was pre-dried in vacuum oven at 100°C for 48 hours and PP was dried at 80°C for 24 hours and SEBS-g-MAH was dried for 8 hours at 60°C. PET, PP, SEBS-g-MAH, and GNP with various amounts of GNP, as summarized in Table II, were melt

Table II. Sample Formulations of GNP-Filled PET/PP Nanocomposites

Sample name	PET (wt %)	PP (wt %)	SEBS-g-MA (phr)	GNP (phr)
GNP0	70	30	10	0
GNP1	70	30	10	1
GNP2	70	30	10	2
GNP3	70	30	10	3
GNP4	70	30	10	4
GNP5	70	30	10	5

blended using a counter-rotating twin screw extruder Plastic Corder, PL 2000. The temperature setting from the hopper to the die was 265/275/280/285°C and the screw speed was 60 rpm. The extruded material was pelletized and then dried at 80°C for 12 hours before injection in an injection moulding (JSW 100 Ton). The temperatures from the hopper to the nozzle were 225–270°C. Standard test samples (ASTM standards) were produced for tensile and impact tests. All tests were conducted more than 24 hours after injection.

CHARACTERIZATIONS

Mechanical Properties

Neat blend and composite tensile bars were tested using a universal tensile tester 20 kN, instrument according to ASTM D 638 standard at a cross-head speed of 50 mm/min. five specimens from each composition were tested along with neat blend specimens for comparison. Notched Izod impact test (ASTM D256) was performed using Izod Toyoseiki (11 J) impact tester at ambient temperature.

Morphological Analysis

Dispersion of the graphene nanoplatelets was observed using field emission scanning electron microscopy (FESEM) and transmission electron microscopy (TEM). FESEM micrographs of fractured surfaces of the neat PET/PP blend and PET/PP GNP composites were obtained using a Hitachi S-4800. The neat blend control and the composites were gold coated using a Balzers Union MED 010 coater. Thin sections (thickness of 70 nm) used for transmission imaging were microtomed using Reichert Jung Ultracut E microtome. Transmission micrographs were collected using a JEOL JEM-2100 microscope, with an operating voltage of 200 kV.

X-ray Diffraction

X-ray diffraction (XRD) patterns were collected using X'Pert, X-ray diffractometer (SIEMENS XRD D5000), and Ni-fltered Cu Kα radiation at an angular incidence of 0°–80° (2θ angle range). XRD scans of the GNP powder along with the composites samples were collected at 40 kV and 50 mA with an exposure time of 120 s.

Fourier Transform Infrared Spectroscopy

To study the interaction between GNP and the matrix, Fourier transform infrared spectroscopy (FTIR) was performed using a Perkin Elmer 1600 infrared spectrometer using the KBr method in the ratio of 1:100 and made to a thin pellet. FTIR spectra of the coated pellet were recorded using a Nicolet AVATAR 360 at 32 scans with a resolution of 4 cm^{-1} and within the wave number range of 370–4000 cm^{-1}. The positions of significant transmittance peaks were determined by using the "find peak tool" provided by the Nicolet OMNIC 5.01 software.

RESULTS AND DISCUSSION

Morphological Analysis

Field Emission Scanning Electron Microscopy. Impact-fractured surface morphologies of PET/PP blends uncompatibilized and compatibilized with SEBS-g-MAH are shown in Figure 1(a,b). The effect of compatibilization can be seen clearly by comparing the morphologies with and without compatibilizer. Without the compatibilizer (Figure1a) the blend shows a brittle type of fracture with the dispersed PP phase having a spherical shape. Larger agglomerated PP particles are also seen against the PET domains. The smooth craters observed in the PET matrix are due to the detached PP particles as occurred during fracture. This presents a clear two-phase morphology of incompatible polymer blends with poor adhesion between the two phases. Similar observation was made by Heino et al.[31] With the addition of 10 phr SEBS-g-MAH as a compatibilizer, ductile fracture is observed indicating effective compatibilization by the elastomeric SEBS-g-MAH (Figure 1b). The toughening of

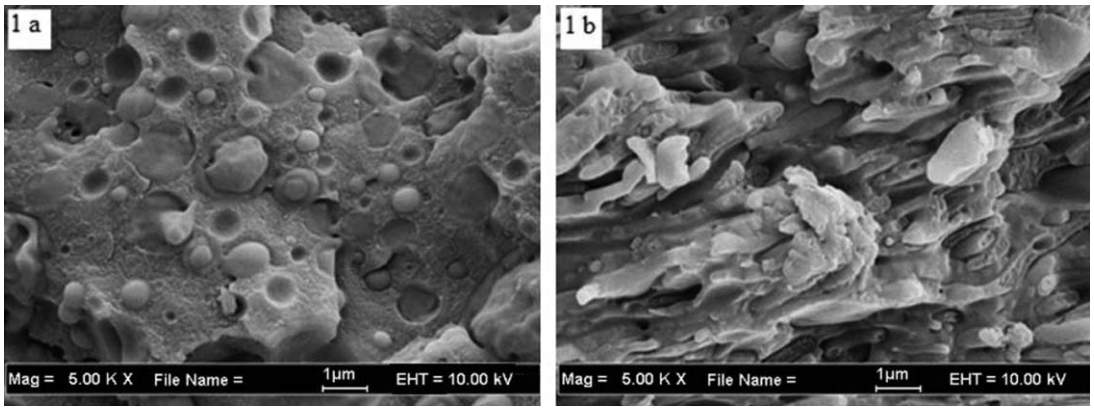

Figure 1. Typical FESEM of impact fractured PET/PP specimen (a) uncompatibilized showing brittle fracture and (b) compatibilized with 10 wt % of SEBS-g-MAH showing a ductile fracture.

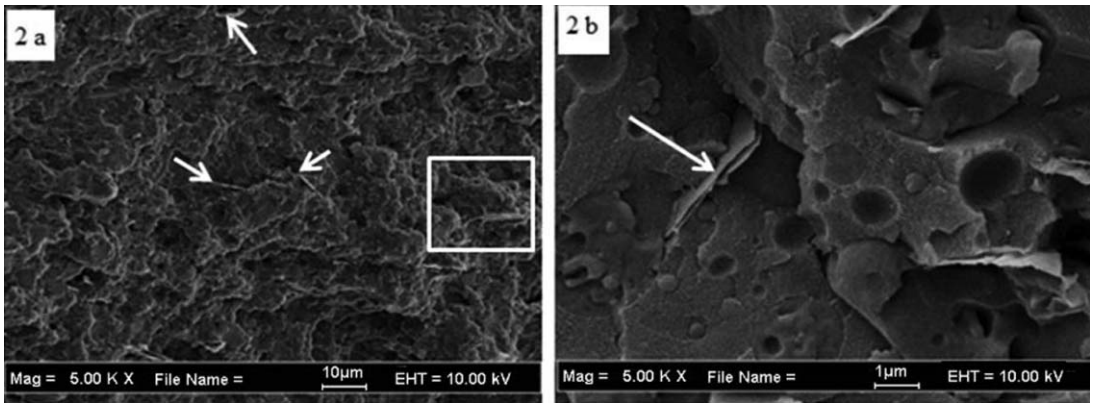

Figure 2. FESEM micrograph of impact fractured surface of graphene-filled (3 phr) PET/PP composite (a) at low magnification and (b) magnified section of (a).

PET/PP blend by SEBS-g-MAH was reported in a previous publication.[30]

The composites were prepared by melt compounding of the GNP powder and the polymer matrices in a single-step process after rigorous premixing to ensure homogenous dispersion of the GNP powder. Figure 2(a,b) shows the micrographs of the composites' fractured surface at 3 phr GNP. It can be seen that the platelets were intact and dispersed into the blend matrix, with no signs of agglomeration at 3 phr. GNP sheets can be seen projecting out of the fractured surface (arrow). They appear to be mixed with the matrix. Similar observation was made by Al-Jabareen et al.[32] The uniform dispersion of GNP in the matrix at this filler concentration is thought to be responsible for the enhancement of tensile and impact strengths as shown in later discussion. Jiang and Drzal[16] studied the morphology of GNP reinforced high-density polyethylene; they observed that both the two types of GNP particles sizes (xGnP1 and xGnP15) were well dispersed in the polymer matrix with the GNP particles embedded in the matrix, indicating an increased adhesion between the filler and matrix. Similarly, Kim et al.[33] reported a uniform dispersion of GNP in LLDPE using three different screw systems and attributed the improved tensile properties to the well-dispersed GNPs in the matrix.

Transmission Electron Microscopy. The properties of nano-sized composite materials are closely related to the extent of dispersion of nanoparticles in the matrix and hence to their effectiveness in enhancing the properties of the nanocomposites, such as mechanical, thermal, and electrical properties. TEM micrographs were collected from 70 nm thin sections to gain better understanding of nanoplatelet dispersion. Figure 3(a,b) depicts the micrographs of the thin section of sample at 3 phr. Apparently, as can be seen in the figure, the presence of multilayer graphene sheets is established, forming a continuous interconnected network. This is evident of homogenous dispersion of GNPs in the blend matrix. Figure 3b shows a graphene nanoplatelet folding due to thin thickness of the sheets and strong shear it was subjected to during composite melt processing in extruder equipment but still remaining intact. This observation is consistent with previous work by Kuila et al.[6] It has been reported that the presence of folded or crumpled graphene sheets may actually lead to nanoscale surface roughness, which would produce an enhanced mechanical interlocking and adhesion with the polymer chains.[34] Although the GNPs were homogenously dispersed in the matrix, full exfoliation has not been substantially achieved for this system using the direct melt processing. Nonetheless, the stiffness of GNPs has contributed to the observed increase in mechanical properties.

X-ray Diffraction. XRD is an effective method to evaluate the interlayer changes of graphite-related powders and crystalline properties of composites. The XRD patterns of the pristine GNP powder, neat PET/PP blend, and PET/PP/GNP composites are shown in Figure 4. The diffraction pattern for the graphene nanoplatelets shows the graphene-2H characteristic peaks at 26.6° (d = 3.35Å) and 54.7° (d = 1.68Å) 2θ. Absence of the characteristic graphene peaks in the nanocomposites indicates the existence of disordered GNPs sheets or long range ordered in the matrix. This observation along with TEM and FESEM images confirms that the GNPs in the composites were not substantially exfoliated. Similar observation was made by Bandla and Jay[27] in the analysis of micrographs of PET/GNP composites.

Fourier Transform Infrared Spectroscopy. To observe any chemical changes occurring, the samples were analyzed using FTIR spectroscopy. Figure 5 shows the FTIR spectra of GNPs powder, neat blend, and PET/PP/GNP composites. No visible peaks were observed in the spectrum of GNPs. This is consistent with the findings of Geng et al.[35] The absence of graphite and graphite oxide peaks confirms the purity of graphene sheets in the GNP powder. These peaks are at 3400 cm^{-1} (O—H stretching vibrations), 1720 cm^{-1} (C═O stretching vibrations), 1220 cm^{-1} (C—OH stretching), and 1060 cm^{-1} (C—O stretching).[36,37] The broad absorption band at 3435 cm^{-1} in the neat blend and the composites is attributed to the hydroxyl group in PET.[38] The peaks at 2923 cm^{-1} appearing in both blend and composites is due to SEBS group in the blend.[21] The peaks at 1610–1722 cm^{-1} characterize the C═O stretching vibrations existing in both PET and maleic anhydride groups, which overlapped indicating good compatibility between the compatibilizer and PET/PP blend that occurred through the interaction of the polar group of the anhydride with the ester group of PET.

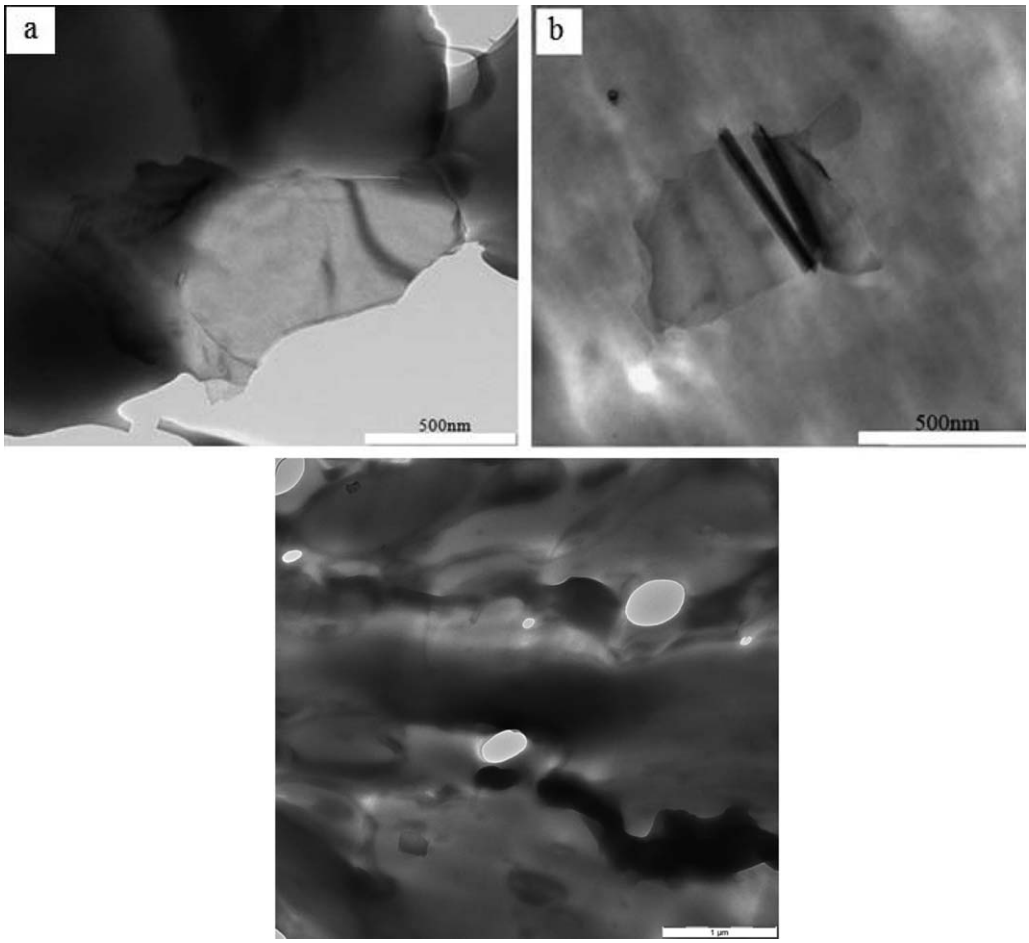

Figure 3. (a) TEM image showing the edge to edge contact of GNP sheets in PET/PP/GNP composites at 3 phr loading; (b) folded graphene sheet; and (c) low magnification showing the dispersion of GNPs in the blend.

Similar observation was made by Chiu et al.[39]. This has corroborated the observation in Figure 1b. The peak at 723 cm^{-1} is attributed to unsaturated C—H stretching vibration. The foregoing discussion indicated that there is no any chemical interaction between GNPs and blend matrix due to the absence of structural changes in the composites. Therefore, any property improvements of the composites are the result of the physical interactions (which improved the adhesion of GNPs to the

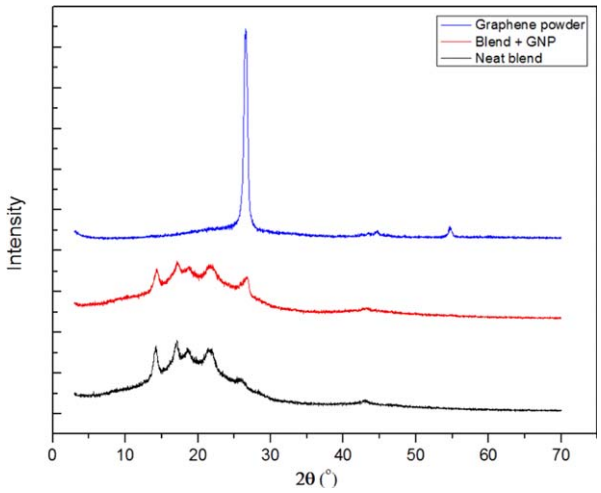

Figure 4. X-ray diffraction features of the PET/PP blends and PET/PP/GNP composites. [Color figure can be viewed in the online issue, which is available at wileyonlinelibrary.com.]

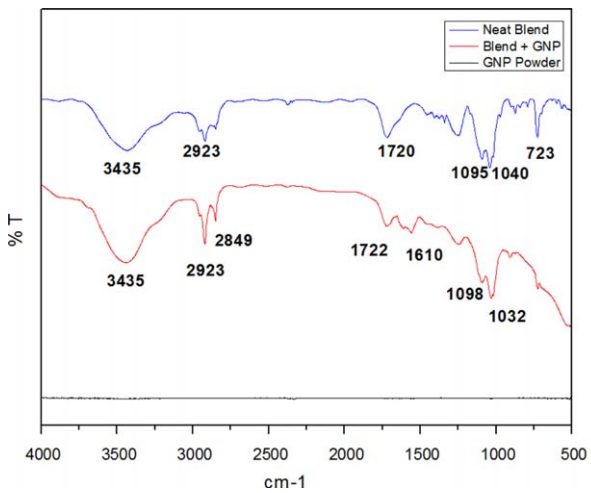

Figure 5. Typical FT-IR of the GNP powder, PET/PP blend and PET/PP/GNP composites. [Color figure can be viewed in the online issue, which is available at wileyonlinelibrary.com.]

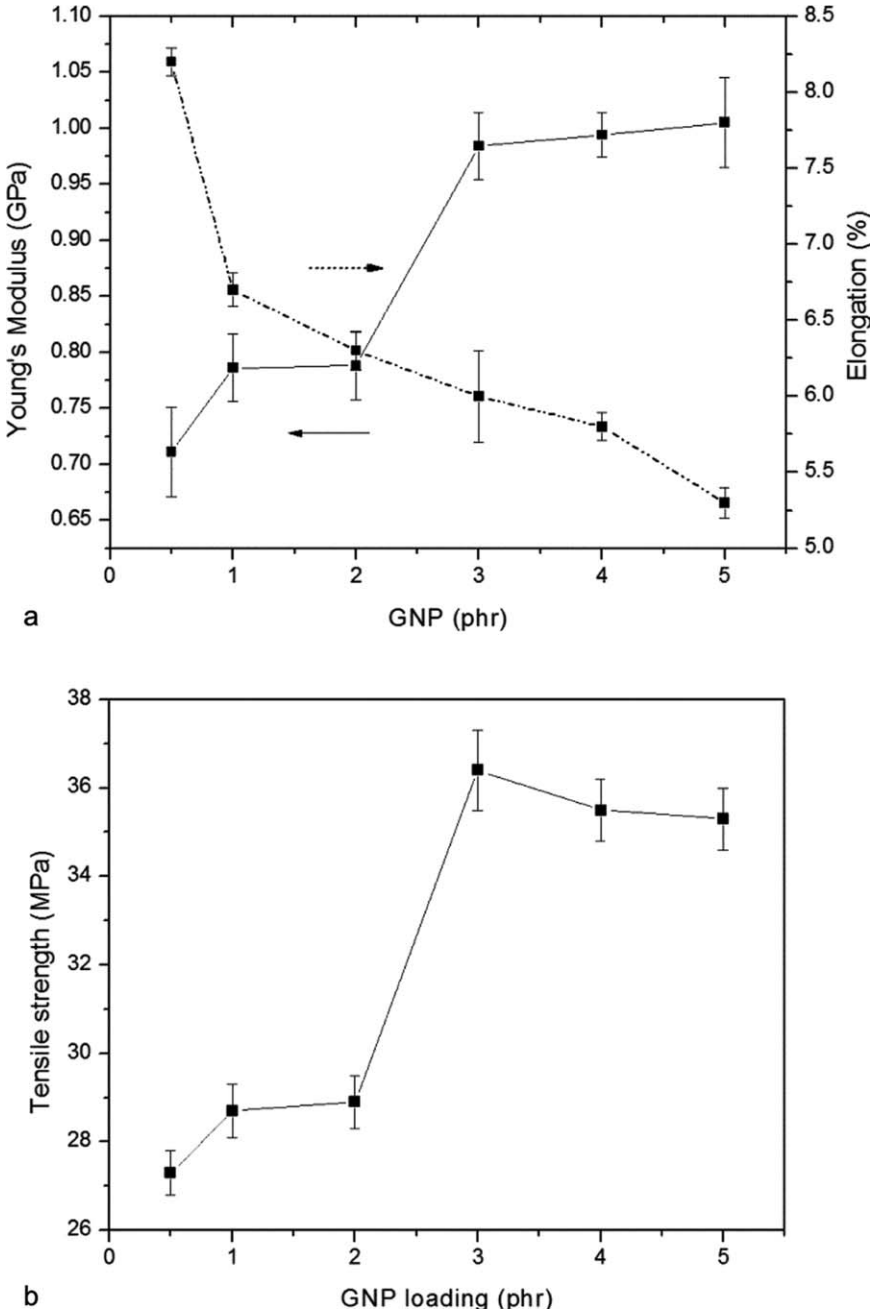

Figure 6. Effect of GNP loading on tensile properties of PET/PP/GNP composites: (a) showing Young's modulus and elongation at break and (b) tensile strength.

matrix) only between the GNPs and the matrix. Similar conclusion was arrived at by Patole et al.[40] They reported that there was no any significant change in peak positions of graphene/polystyrene composites compared with pristine/polystyrene nanoparticles.

Mechanical Properties

Tensile Properties. The extent of nanofiller dispersion in the polymer matrix is directly related to its effectiveness for improving properties of composite.[8] The effect of GNP loading on young's modulus, elongation at break, and tensile strength is shown in Figure 6. The Young's modulus increases linearly with the GNP loading (Figure 6a), from a value of 1.4 GPa for neat blend to 1.9 GPa for 5.0phr GNP loading. This behavior is attributed to effective stress transfer between matrix and filler arising from uniform dispersion of the nanoplatelets. Mohamadi et al.[41] reported improvement in Young's modulus of PDVF/PMMA blend (70:30) by more than 20% due to the addition and dispersion GNPs in the blend. Figure 6a shows a gradual decrease in elongation at break with GNP loading. The elongation decreased from 15% for neat blend to 2.3% for 5.0 phr GNP loading. The decrease is attributed to restrictions in segmental chain movement with increasing graphene content due to interaction of polymer matrix with the stiffer GNP. This

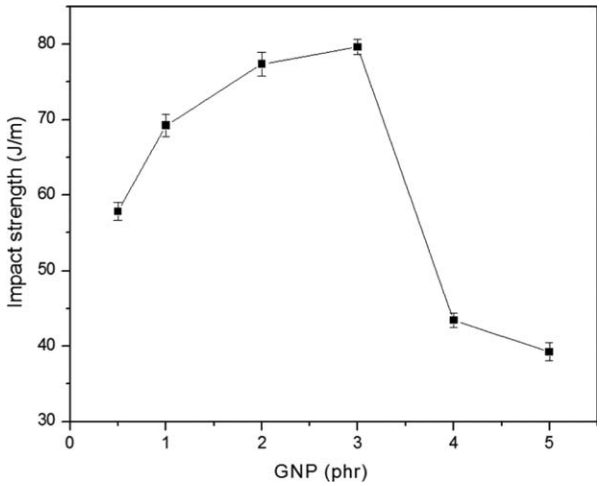

Figure 7. Effect of GNP loading on impact strength of PET/PP/GNP composites.

finding is consistent with the report by Kim and Jeong[42] in which they observed a decrease in percent strain at break of polylactide/exfoliated graphite nanocomposites with GNP loading. On the contrary, the tensile strength reaches a maximum at 3.0 phr loading (Figure 6b). Previous studies on GNP-reinforced polymer nanocomposites show that tensile strength goes up to a peak value at a critical concentration, and then goes down with further GNP loading.[43,44] It is assumed that further addition of GNP into the polymer, the phenomenon of graphene restacking, occurs due to van der Waals attraction between the nanoplatelets. Slippage of piled graphene sheets during tensile test will have less effective enhancement on the strength.[8]

Impact Strength. Figure 7 shows the effect of GNP loading on impact strength of PET/PP/GNP composites. A reduction in impact strength was observed in all composites compared to the neat blend. The decrease in impact strength of the composites compared to the neat blend can be attributed to incompatibility between the matrix and filler and also the heterogeneous nature of the PET/PPGNP nanocomposites. Similar trend is reported by Wang et al.[43] in a study to compare GNPs and carbon black on the mechanical properties of HDPE. Li and Chen[45] also reported a reduction of impact strength of HDPE/expanded graphite nanocomposites prepared via masterbatch process compared with pure HDPE due to the presence of the graphene layers in the matrix. However, as can be seen in the figure, PET/PP/GNP composites exhibit the least reduction of impact strength at 3 phr loading. This corresponds to the optimum filler concentration in which uniform dispersion of GNPs was achieved. Differences in dispersion situation among the different loadings may result in different energy-absorbing mechanisms at the impact fracture surface.[16]

The sharp drop of impact strength after 3 phr is attributed to the restacking phenomenon discussed earlier. Figure 8 is a proposed scheme of GNP dispersion in polymer matrix as postulated by Zhao et al.[8] It is proposed here that at low concentration the GNP nanoparticles are individually dispersed in the polymer matrix at intervals. At higher concentration, the edges of the platelets just joined together side by side. This condition is presumed to correspond with 3.0 phr GNP loading and is the ideal condition exhibiting ultimate contribution to the mechanical behavior with the greatest efficiency.

According to the experimental results, the optimum loading of GNP in PET/PP/ blend is 3 phr. When the GNP concentration is increased beyond the optimum level (3 phr), the platelets begin to overlap on one another as illustrated in Figure 8. At higher loading, the platelets start restacking together in layers owing to strong van der Waals forces and $\pi \rightarrow \pi$ attraction between GNP planes and the small distance between the graphene sheets. Filler–filler interaction is presumed to be

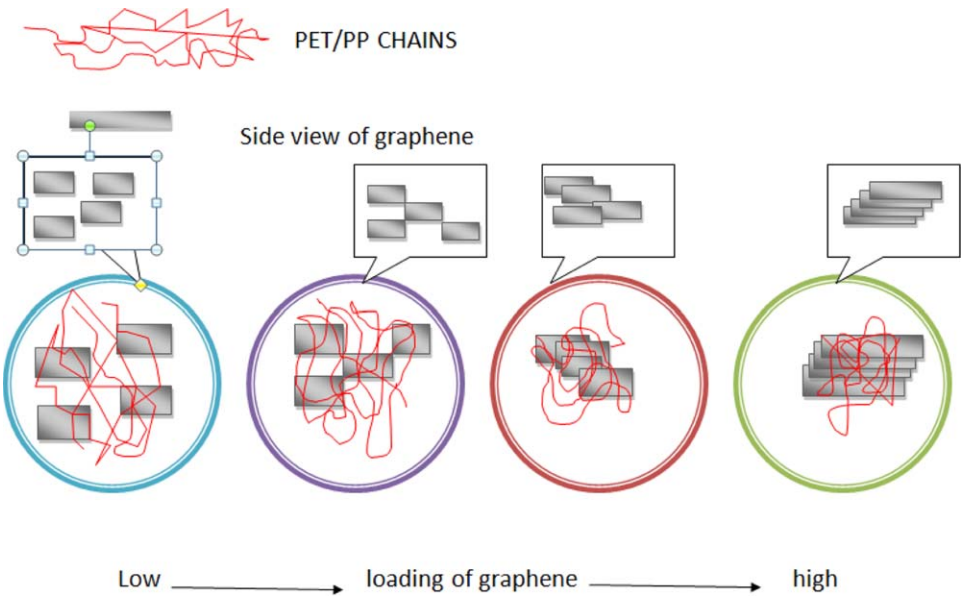

Figure 8. Illustrated scheme of GNP dispersion situations in PET/PP matrix. [Color figure can be viewed in the online issue, which is available at wileyonlinelibrary.com.]

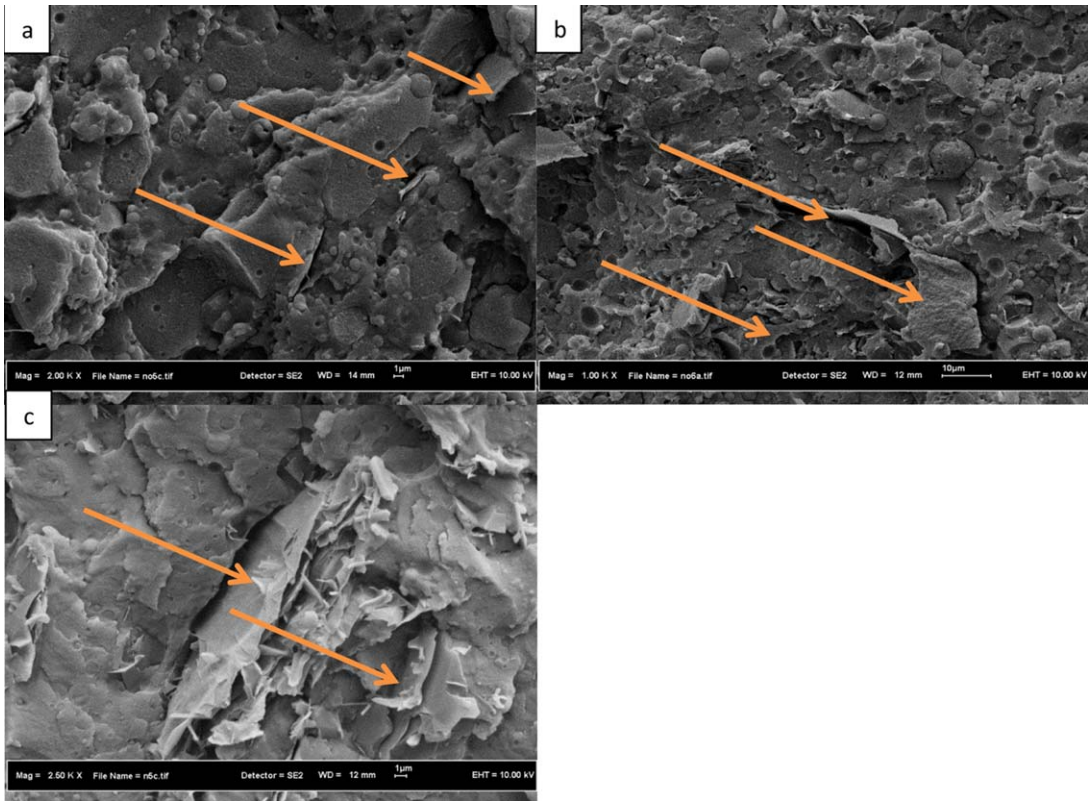

Figure 9. Differences in the dispersion situation of GNP content on the morphology of PET/PP/GNP composites (a) low GNP content; (b) GNP begin to overlap at high content; and (c) restacking of GNPs due to van Der Waals force and $\pi \rightarrow \pi$ attraction. [Color figure can be viewed in the online issue, which is available at wileyonlinelibrary.com.]

responsible for the observed decrease in mechanical properties of the composites beyond the 3 phr concentration. This observation is depicted in Figure 9 using FESEM images. At low filler loading (Figure 9a), individual GNPs are scattered with no contact (stage 1), while overlapping started at higher GNP loading (Fig 9b) (stage 3). Agglomerated GNPs can be seen in Figure 9c (stage 4) corresponding to a fully stacked GNPs due to van der Waals forces and $\pi \rightarrow \pi$ attraction, which are the main bane to GNPs' dispersion in polymer matrix. This corresponds to 5 phr loading in which case both the tensile and impact strengths have declined.

CONCLUSION

Exfoliated GNP-reinforced PET/PP composites were prepared by melt-blending technique. FTIR spectroscopy did not show any significant changes in peak positions of PET/PP/GNP spectrum compared with PET/PP neat blend, which indicated lack of strong chemical interaction between GNP and the blend matrix. Evidence from TEM, FESEM, and XRD showed that the platelets remain intact and dispersed homogenously in the polymer matrix without substantial exfoliation of GNPs in the polymer matrix. Improvements in tensile strength and impact strength of the composites were observed up to 3phr filler loading with corresponding decrease in elongation at break. The improvements observed in mechanical properties are attributed to stiffness of the platelets and effective stress transfer between matrix and filler.

ACKNOWLEDGMENTS

The authors thank the Ministry of Higher Education of Malaysia (MOHE) and Universiti Teknologi Malaysia (UTM) for Research Universiti Grant vote number 02H26 and sub code Q.J130000.7113.02H26.

REFERENCES

1. Liu, X.-G. *Carbon.* **2013**, *51*, 438.
2. Geim, A. K.; Novoselov, K. S. *Nat. Mater.* **2007**, *6*, 183.
3. Lee, C.; Wei, X.; Kysar, J.W.; Hone, J. *Science.* **2008**, *321*, 385.
4. Gómez-Navarro, C.; Weitz, R. T.; Bittner, A. M.; Scolari, M.; Mews, A.; Burghard, M.; Kern, K. *Nano Lett.* **2007**, *7*, 3499.
5. Alexander, A. B.; Ghosh, S.; Wenzhong, B.; Calizo, I.; Teweldebrhan, D.; Miao, F.; Lau, C. N. *Nano Lett.* **2008**, *8*, 902.
6. Kuila, T.; Saswata, B.; Khanra, P.; Hoon, K., N.; Rhee, K. Y.; Lee, J. H. *Compos. Part A: Appl. Sci. Manufact.* **2011**, *42*, 1856.
7. Kuila, T.; Saswata, B.; Khanra, P.; Mishra, A. K.; Khanra, P.; Lee, N. H.; Hee, *J. Polym. Test.* **2012**, *31*, 31.
8. Zhao, X.; Qinghua, Z.; Chen, D.; Ping, L. *Macromolecules.* **2010**, *43*, 2357.
9. Rafiee, M. A.; Rafiee, J.; Wang, Z.; Song, H.; Yu, Z.-Z.; Koratkar, N. *ACS Nano.* **2009**, *3*, 3884.

10. Bandla, S., Hanan, J. C., *J. Mater. Sci.* **2012**, *47*, 876.
11. Kalaitzidou, K.; Hiroyuki, F.; Miyagawa, H.; Lawrence, T. D. *Polym. Eng. Sci.* **2007**, *47*, 1796.
12. Kalaitzidou, K.; Fukushima, H.; Drzal, L. T. *Compos. Part A: Appl. Sci. Manufact.* **2007**, *38*, 1675.
13. Bandla, S., Hanan, J. C. ANTEC **2011**, Boston. pp 673.
14. Persson, H.; Yao, Y.; Klement, U.; Rychwalski, R. W, *eXPRESS Polym. Lett.* **2012**, *6*, 5.
15. Li, M.; Jeong, Y. G., *Compos. Part A: Appl. Sci. Manufact.* **2011**, *42*, 560.
16. Jiang, X. D.; Lawrence T. *Polym. Compos.* **2010**, *31*, 1091.
17. Kalaitzidou, K. *Exfoliated Graphite Nanoplatelets as Reinforcement for Multifunctional Polypropylene Nanocomposites*, Michigan State University, **2006**.
18. Fasihi, M.; Garambi, H.; Ghaffarian, S. R.; Ohshima, M. *J. Appl. Polym. Sci.* **2013**, *130*, 1834.
19. Bian, J.; Wei, X. W.; Lin, H. L.; Wang, L.; Guan, Z. P. *J. Appl. Polym. Sci.* **2012**, *124*, 3547.
20. Kale, E. Available at: http://www.tgdaily.com/general-sciences-features/78573-the-eco-friendly-car-is-driving-engineering-plastics-market-to-76-bi#VRkDTSm6J5LpjbcK.99; Ed.; **2013**.
21. Tanrattanakul, V.; Hiltner, A.; Baer, E.; Perkins, W. G.; Massey, F. L.; Moet, A. *Polymer.* **1997**, *38*, 2191.
22. Tanrattanakul, V.; Hiltner, A.; Baer, E.; Perkins, W. G.; Massey, F. L.; Moet, A. *Polymer.* **1997**, *38*, 4117.
23. Loyens, W.; Groeninckx, G. *Polymer.* **2002**, *43*, 5679.
24. Chan, C.-M.; Jingshen, W.; Li, J.-X.; Cheung, Y.-K. *Polymer.* **2002**, *43*, 2981.
25. Wen, X.; Wang, Y.; Gong, J.; Liu, J.; Tian, N.; Wang, Y.; Jiang, Z.; Qiu, J.; Tang, T. *Polymer Degrad. Stab.* **2012**, *97*, 793.
26. Zhang, H.-B.; Zheng, W.-G.; Yan, Q.; Yang, Y.; Wang, J.-W.; Lu, Z.-H.; Ji, G.-Y.; Yu, Z.-Z. *Polymer.* **2010**, *51*, 1191.
27. Bandla, S.; Hanan, J. *J. Mater. Sci.* **2012**, *47*, 876.
28. Calcagno, C. I. W.; Miriani, C. M.; Teixeira, S. R.; Mauler, R. S. *Compos. Sci. Technol.* **2008**, *68*, 2193.
29. Farimani, H. E.; Ebrahimi, N. G. *J. Appl. Polym. Sci.* **2012**, *124*, 4598.
30. Abdul Razak, N. C.; Inuwa, I. M.; Hassan, A.; Samsudin, S. A. *Compos. Interf.* **2013**, *20*, 507.
31. Heino, M.; Kirijava, J.; Hietaoja, P.; Seppala, J. *J. Appl. Polym. Sci.* **1997**, *65*, 241.
32. Al-Jabareen, A.; Al-Bustami, H.; Hannah, H., Marom, G. *J. Appl. Polym. Sci.* **2013**, *128*, 1534.
33. Kim, S.; Do, I.; Drzal, L. T. *Macromol. Mater. Eng.* **2009**, *294*, 196.
34. Ramanathan, T.; Abdala, A. A.; Stankovich, S.; Dikin, D. A.; Herrera-Alonso, M.; Piner, R. D.; Adamson, D. H.; Schniepp, H. C.; Chen, X.; Ruoff, R. S.; Nguyen, S. T.; Aksay, I. A.; Prud'homme, R. K.; Brinson, L. C., *Nat. Nanotechnol.* **2008**, *3*, 327.
35. Geng, Y.; Wang, S. J.; Kim, J.-K. *J. Coll. Interf. Sci.* **2009**, *336*, 592.
36. Tapas, K.; Saswata, B.; Hong, C. E.; Uddin, Md E.; Khanra, P.; Kim, N. H.; Lee, J. H. *Carbon.* **2011**, *49*, 1033.
37. Xu, Z.; Gao, C. *Macromolecules.* **2010**, *43*, 6716.
38. Yu, Z. Z.; Yang, M. S.; Dai, S. C.; Mai, Y. W. *J. Appl. Polym. Sci.* **2004**, *93*, 1462.
39. Chiu, H. T.; Hsiao, Y. K. *J. Polym. Res.* **2006**, *13*, 153.
40. Patole, A. S.; Patole, S.P.; Kang, H.; Yoo, J.-B.; Kim, T.-H.; Ahn, J.-H., *J. Coll. Interf. Sci.* **2010**, *350*, 530.
41. Mohamadi, S.; Sharifi-Sanjani, N.; Foyouhi, A. *J. Poly. Res.* **2013**, *20*, 46.
42. Kim, I.-H.; Jeong, Y. G., *J. Poly. Sci. Part B.* **2010**, *48*, 850.
43. Wang, L.; Hong, J.; Chen, G., *Polym. Eng. Sci.* **2010**, *50*, 2176.
44. Min, C.; Demei, Y. *Polym. Eng. Sci.* **2010**, *50*, 1734.
45. Li, Y.-C.; Guo-Hua, C. *Polym. Eng. Sci.* **2007**, *47*, 882.